GDE2 regulates subtype specific motor neuron generation through inhibition of Notch signaling

Priyanka Sabharwal[1], **Changhee Lee**[1], **Sungjin Park**[1], **Meenakshi Rao**[1,2], and **Shanthini Sockanathan**[1,*]

[1]The Solomon Snyder Department of Neuroscience, The Johns Hopkins University, School of Medicine, PCTB1004, 725 N Wolfe Street, Baltimore, MD 21205. Phone: (410) 502-3084; Fax: (410) 614-8423

Abstract

The specification of spinal interneuron and motor neuron identities initiates within progenitor cells, while motor neuron subtype diversification is regulated by hierarchical transcriptional programs implemented postmitotically. Here, we find that mice lacking GDE2, a six-transmembrane protein that triggers motor neuron generation, exhibit selective losses of distinct motor neuron subtypes, specifically in defined subsets of limb-innervating motor pools that correlate with the loss of force-generating alpha motor neurons. Mechanistically, GDE2 is expressed by postmitotic motor neurons but utilizes extracellular glycerophosphodiester phosphodiesterase activity to induce motor neuron generation by inhibiting Notch signaling in neighboring motor neuron progenitors. Thus, neuronal GDE2 controls motor neuron subtype diversity through a non cell-autonomous feedback mechanism that directly regulates progenitor cell differentiation, implying that subtype specification initiates within motor neuron progenitor populations prior to their differentiation into postmitotic motor neurons.

Introduction

The mechanisms that control neuronal diversity are complex and involve a constant interplay between extrinsic signaling pathways and intrinsic cell-autonomous molecular networks (reviewed in Dasen and Jessell, 2009; Dehay and Kennedy, 2007). These processes operate at different stages of the cell-cycle according to cellular context such that neuronal fate can be specified within the last cell division cycle of progenitors or within postmitotic neurons themselves. While the events that govern and distinguish the identities of distinct neuronal classes are beginning to be understood, the mechanisms that impose subtype diversity within a single class of neurons are not as clear.

One system where this question has been extensively studied is in developing spinal motor neurons (Dasen and Jessell, 2009). The complexity and range of motor behaviors requires the coordinate activation of multiple muscle groups, each of which is innervated by specific groups of motor neurons. Individual motor neuron groups are highly organized in terms of their cell body distribution, projection patterns and function, and consist of force-generating

alpha motor neurons that innervate extrafusal muscle fibers and stretch-sensitive gamma motor neurons that innervate intrafusal muscle fibers of the muscle spindles (Dasen and Jessell, 2009; reviewed in Kanning et al., 2010). The integration of input from both alpha and gamma motor neurons is essential for coordinated motor movement to occur (Kanning et al., 2010).

How is diversity engendered in developing motor neurons? All motor neurons initially derive from ventral progenitor cells that are specified to become Olig2$^+$ motor neuron progenitors through shh and retinoic acid (RA) signals (Novitch et al., 2003; Diez del Corral et al., 2003). Postmitotic motor neuron generation from Olig2$^+$ progenitors is governed by RA through the induction of GDE2, a six transmembrane protein with an extracellular glycerophosphodiester phosphodiesterase (GDPD) domain (Novitch et al., 2003; Diez del Corral et al., 2003; Rao and Sockanathan, 2005, Yan et al., 2009; Nogusa et al., 2004). GDE2 is expressed in all somatic motor neurons and synchronizes neurogenic and motor neuron fate specification pathways to drive motor neuron generation through extracellular GDPD activity (Rao and Sockanathan, 2005, Yan et al., 2009). Newly generated motor neurons share generic motor neuron properties that are distinct from neighboring interneurons, for example their use of acetylcholine as a neurotransmitter and the ability of their axons to exit the ventral root. Postmitotic motor neurons subsequently diversify into different motor columns and pools that have distinct positional, molecular and axonal projection profiles that are fundamental to motor circuit formation (Dasen and Jessell, 2009). The major motor columns in the spinal cord consist of the Median Motor Column (MMC), which spans the entire body axis and innervates dorsal axial muscles; the preganglionic (PGC) and hypaxial motor columns (HMC) located primarily at thoracic levels, which respectively target the viscera and body wall muscles (Prasad and Hollyday, 1991); and the limb-specific Lateral Motor Columns (LMC), which are divided into lateral and medial subdivisions that innervate dorsal and ventral limb musculature (Landmesser, 1978; Landmesser, 2001). Medial and lateral LMC motor neurons are further clustered into motor pools according to their projections to individual target muscles (Gutman et al., 1993; Landmesser 1978; Lin et al., 1998).

Current models propose that columnar and pool identities are instructed in newly born motor neurons via intrinsic hierarchical transcription programs and extrinsic signals. The distinction between MMC and non-MMC motor columns is imposed via ventrally-derived Wnt signals (Agalliu et al., 2009), while non-MMC motor columnar identity is directed by early mesodermal sources of graded FGF, retinoid and TGFβ–like signals. These pathways ultimately regulate the motor neuron specific expression of Hox transcription factors in restricted rostral-caudal domains where they regulate the expression of transcription factors such as the LIM homedomain proteins to specify the settling position and axonal projection patterns of prospective LMC and PGC neurons (Dasen and Jessell, 2009, Ji et al., 2009; Shah et al., 2004; Wu et al., 2008; Jung et al., 2010). Hox proteins play principal roles in the formation of motor pools spanning the LMC and within a single spinal segment (Dasen et al., 2005); however they are not the sole regulators of motor pool identity. Target-derived signals induce the expression of ETS transcription factors such as ER81 and Pea3 within a select subset of motor pools, which subsequently dictate and refine sensorimotor connectivity (Lin et al., 1998; Arber et al., 2000; Haase et al., 2002; Vrieseling and Arber, 2006). Interestingly, alpha and gamma motor neurons appear identical in terms of their gene expression, morphology, and peripheral projections during embryogenesis (Burke, 1977; Friese et al., 2009; Kanning et al., 2010). These observations suggest that they initially undergo comparable programs of column and pool-specific differentiation but diverge prenatally to acquire their individual properties (Friese et al., 2009, Shneider et al., 2009).

The evidence thus far suggests that in contrast to the mechanisms that instruct the differentiation of different neuronal subclasses within the spinal cord, subtype diversification amongst motor neurons appears to operate postmitotically (Dasen and Jessell, 2009). However, the ability of certain Hox proteins to influence motor columnar identity through their function in progenitors and observations from neural tube rotation experiments that suggest that motor pool fates are specified at the time of motor neuron progenitor differentiation, raise the possibility that motor neuron subtype diversity is initiated within motor neuron progenitors (Dasen et al., 2003; Matise and Lance-Jones, 1996). In support of this model, we provide here genetic evidence suggesting that newly-born motor neurons are not uniform as previously believed but are biased from the outset towards particular fates. We show that GDE2 does not regulate the generation of all motor neurons but is required for the timing and generation of distinct LMC motor pools in particular, their alpha motor neuron components. Mechanistically, we show that GDE2 regulates motor neuron differentiation by antagonizing Notch signaling in neighboring motor neuron progenitors through extracellular GDPD activity. These observations define GDE2 as a key regulator of motor neuron diversity through its function in regulating motor neuron progenitor differentiation, and suggest that fundamental distinctions between different motor neuron subtypes are imposed earlier than previously appreciated, namely within motor neuron progenitors prior to their differentiation into postmitotic motor neurons.

Results

GDE2 expression in spinal motor neurons

GDE2 is expressed in motor neurons at all axial levels (Rao and Sockanathan, 2005). To define the developmental profile of *Gde2* expression we examined the distribution of *Gde2* transcripts in embryonic forelimb spinal cords from E9.5 when motor neurons are first generated, to E12.5 when motor columns have been established. *Gde2* mRNA is detected in somatic motor neurons until E11.5 but is substantially decreased by E12.5 (Figure 1A–D; data not shown). Consistent with previous studies showing a requirement for GDE2 in interneuron generation, *Gde2* transcripts extend dorsally from E10.5 coincident with the timing of ventral and dorsal interneuron formation (Figure 1B, C; Yan et al., 2009). Similarly, GDE2 protein is expressed in postmitotic somatic motor neurons from E9.5, and detected dorsally from E10.5 (Figure 1E–F). Examination of GDE2 expression in relation to columnar-specific motor neuron markers at fore- and hindlimb levels of the spinal cord shows that GDE2 is localized to newly differentiating motor neurons and to MMC and lateral and medial LMC motor neurons (Figure 1E–G′; data not shown; Tsuchida et al., 1994). By E12.5, GDE2 protein is reduced within motor neuron cell bodies but is enriched within motor axons, suggesting that GDE2 may have later roles in postmitotic motor neuron development (Figure 1H, I). Thus, GDE2 is expressed in somatic motor neuron cell bodies coincident with the period of motor neuron neurogenesis.

GDE2 is required for motor neuron formation

To test the requirement for GDE2 in regulating motor neuron generation, we generated stable mouse lines that lack functional GDE2 ($Gde2^{-/-}$) using Cre-lox technology (Figure S1). We confirmed GDE2 ablation using a combination of PCR, direct sequencing, Western blot and immunohistochemical analyses (Figure 7C, Figure S1). Examination of $Gde2^{-/-}$ and WT littermates at the onset of motor neuron differentiation at E9.5 showed an approximately 50% loss of $Isl1/2^+$ and $HB9^+$ motor neurons (Figure 2A, B, D, E, G; Nornes and Carry, 1978). However, the number of $Olig2^+$ motor neuron progenitors and the dorsal-ventral patterning of spinal progenitors were not affected (Figure 2C, F, G; Figure S2). No increase in TUNEL staining was detected in $Gde2^{-/-}$ animals, suggesting that the loss of GDE2 does not compromise motor neuron survival, but instead disrupts motor neuron

formation (Figure S2). Consistent with this model, *Gde2* null mutants showed a decrease in the number of progenitors exiting the cell-cycle (Figure 2J, M, N). Although no changes in the proportion of cells in S-phase and M-phase were detected, the total number of cells in S-phase after a 16 hour BrdU pulse was increased, suggesting that the length of the cell-cycle is extended in the absence of GDE2 (Figure 2H–N; Yan et al., 2009). These data collectively support previous findings in the chick that GDE2 is required to regulate motor neuron generation, but does not affect progenitor patterning and specification (Rao and Sockanathan, 2005).

GDE2 function is restricted to specific motor columns

Some motor neurons are generated in the absence of GDE2 suggesting that GDE2 function might be redundant with its family members *Gde3* and *Gde6* (Nogusa et al., 2004; Yanaka et al., 2003). However, *Gde3* and *Gde6* transcripts do not overlap with *Gde2* mRNA in spinal motor neurons (data not shown). To determine if GDE2 is required for the generation of motor neurons of distinct subtypes, we examined motor column formation in WT and *Gde2* null littermates (Figure S3; Tsuchida et al., 1994; Rousso et al., 2008; Dasen et al., 2008). At fore- and hindlimb levels, *Gde2* null animals showed an approximately 40–50% loss of medial and lateral LMC neurons at E11.5 and a decrease of 30–35% at E13.5 (Figure 3A–G, O–U), whereas we noted a modest decrease of 20% in thoracic HMC neurons at E11.5 (Figure 3H–N). Strikingly, no changes in the numbers of MMC neurons or PGC neurons were found at either timepoint (Figure 3A–U). The loss of HMC and LMC neurons in *Gde2*$^{-/-}$ animals is unlikely to be due to impaired Hox activities because: (1) gain or loss of Hox gene function does not reduce motor neuron numbers, (2) expression of FoxP1, a critical cofactor of Hox function, in existing motor neurons is unaffected by the loss of GDE2 (Figure 3A–T; Rousso et al., 2008; Dasen et al., 2008) and (3) brachial Hoxc6, thoracic Hoxc9 and lumbar Hoxa10 expression are preserved in motor neurons of *Gde2*$^{-/-}$ animals (Figure S3; Jung et al., 2010). V2 interneurons derive from Lhx3$^+$ progenitors and V2 interneuron differentiation programs are actively suppressed in motor neurons by the transcription factor HB9 (Arber et al., 1999; Thaler et al., 1999; Thaler et al., 2002). Islet1/2 motor neurons did not coexpress Chx10, no increases in cell death by TUNEL were detected, and V2 interneuron numbers were unchanged in the absence of GDE2, arguing against the possible conversion of prospective HMC and LMC neurons to V2 fates (Figures S3 and S2; data not shown).

Taken together, these observations suggest that GDE2 function is restricted to the formation of LMC and HMC motor neurons and further, invokes the existence of other regulatory modules that control the formation of GDE2-independent motor neurons.

GDE2 is required for the differentiation of specific motor pools

The loss of fore- and hindlimb LMC neurons in *Gde2*$^{-/-}$ animals indicates that GDE2 activity is not restricted to a specific rostral-caudal domain while the partial reduction of medial and lateral LMC neurons suggests that GDE2 might be required for the formation of distinct LMC motor pools (Figure 3). We analyzed *Gde2* null animals at lumbosacral segment (LS) 2 of the spinal cord, where combined molecular and axonal tracing approaches have defined a molecular code that distinguishes seven medial and lateral LMC motor pools that innervate major muscle groups in the hindlimb (Figure 4C; de Marco Garcia and Jessell, 2007; Lin et al., 1998; Arber et al., 2000). These include five motor pools within the medial LMC that innervate the adductor longus and magnus (Al, Am), the adductor brevis (Ab), and the anterior and posterior gracilis muscles (Ga, Gp); and two lateral LMC pools that target the vasti (Va) and the rectofemoratibialis muscles (Rf). We assigned motor neurons to specific motor pools based on their position along the dorsal-ventral and medial-lateral axes, and by their unique molecular identity in terms of two separate molecular codes (Figure 4C).

Analysis of the LS2 LMC motor pools in *Gde2*$^{-/-}$ animals at E13.5 and E14.5 showed a dramatic reduction of the medial Ga motor pool (dorsal green cells, Figure 4A and B) and a 60–70% reduction of medial Ab motor neurons (Figure 4A–C, E–J, L). Furthermore, we detected a 60–70% reduction in the lateral Va motor pool at E13.5 and E14.5 (Figure 4A–C, I–K), and a 40–50% reduction in the Rf motor pool at E13.5 (Figure 4C, D, M, N). The *bona fide* loss of these motor pools in *Gde2*$^{-/-}$ animals is further substantiated by the absence of Isl2$^+$/Lhx1$^+$ and Foxp1$^+$/Isl2$^+$ lateral LMC motor neurons in adjacent sections; the observation that medial Ab and lateral Va motor neurons could not be detected in *Gde2*$^{-/-}$ animals from the time of Ab and Va motor pool formation at E12.5 and from EdU birthdating studies showing that many Ab and Va motor neurons are not born in the absence of GDE2 (Figure S4; data not shown). Further, TUNEL labeling was equivalent between WT and *Gde2*$^{-/-}$ animals from E9.5 to E14.5, arguing for deficits in motor neuron generation rather than survival in the absence of GDE2 (Figure S2).

In contrast, the numbers of neighboring Al, Am and Gp medial LMC motor neurons were decreased at E12.5 in *Gde2*$^{-/-}$ embryos but were equivalent to controls at E13.5 and E14.5 (Figure 4A–C, G, I, J; Figure S4). Visualization of the major axonal tracts emerging from LS2 using *HB9-GFP* transgenic animals showed that they appeared thinner in *Gde2*$^{-/-}$ animals consistent with a loss in motor neuron numbers (Figure S4; Huber et al., 2005). However, existing LMC neurons showed no obvious deficits in motor axon extension at E12.5 and E14.5 and were capable of forming neuromuscular junctions (Figure S4; data not shown). These observations argue against the possibility that target-derived Pea3 and Er81 expression that mark these pools was delayed due to stunted axonal outgrowth or failure in synaptogenesis (Figure S4; data not shown). Instead, consistent with a delay in their formation, birthdating studies using timed injection of EdU showed that the Al, Am and Gp pools were born later in *Gde2*$^{-/-}$ animals compared with WT littermates (Figure S4).

Taken together, our results suggest that GDE2 regulates the timing of formation of medially located Al, Am and Gp motor pools and is necessary for the generation of prospective Ab, Ga, Va and Rf motor neurons. Our data argue against the likelihood that the loss of motor pools is due to disrupted Hox function as the Al, Am, and Gp motor pools were not expanded as a consequence of Ab, Ga, Va and Rf reduction in *Gde2*$^{-/-}$ animals. Moreover, the expression of the Hox downstream target gene, Nkx6.1, in existing motor neurons is unaffected by GDE2 elimination (Figure 4A–C, G, I, J; de Marco Garcia and Jessell, 2007; Dasen et al., 2003). As motor pools emerge in the context of individual columns, our data suggest that GDE2 controls the formation of motor neurons with specific columnar and pool identities.

GDE2 ablation compromises alpha motor neuron differentiation

We noted that 30–40% of motor neurons are preserved in laterally located LMC motor pools in the absence of GDE2 at E13.5. This number is remarkably similar to that reported for the gamma motor neuron component of motor pools, which are predicted to begin diversifying from alpha motor neurons by E13.5 given their differential sensitivities to embryonic programmed cell death (Burke et al., 1977; Friese et al., 2009; Buss et al., 2006; Hui et al, 2008). To examine if GDE2 selectively regulates the differentiation of alpha but not gamma motor neurons, we compared *Gde2*$^{-/-}$ animals with WT siblings at postnatal day 5 (P5) and P28 when molecular and somal size differences allow alpha and gamma motor neurons to be distinguished (Friese et al., 2009). The percentage of ChAT$^+$/NeuN$^+$ alpha motor neurons in the ventral outer quadrant of the spinal cord corresponding to the LMC was decreased by approximately 30–40% at P5 and P28 in *Gde2*$^{-/-}$ animals; however, the percentage of ChAT$^+$/NeuN$^-$ gamma motor neurons was not significantly altered (Figure 5A–F). The expression of *Err3* in the ventral horn of the spinal cord appeared similar between *Gde2*$^{-/-}$ and WT littermates, consistent with preserved gamma motor neuron differentiation in the

absence of GDE2 (Figure 5G, H). Gamma motor neurons have a small somal area compared with alpha motor neurons (Burke et al., 1977; Friese et al., 2009; Shneider et al., 2009). The number of putative gamma motor neurons (somal area <380μm^2) was unchanged between WT and $Gde2^{-/-}$ littermates but there was a dramatic reduction of putative alpha motor neurons in $Gde2^{-/-}$ animals (somal area = 380–1400μm^2) (Figure 5I, J). Using the same criteria discussed above, no significant changes in alpha and gamma motor neuron numbers were observed in the medially located MMC of $Gde2^{-/-}$ and WT animals (Figure 5M–O).

Thus, the reduction in LMC motor pools in $Gde2$ null animals correlates with a specific loss of alpha motor neurons, while LMC gamma motor neurons and MMC alpha and gamma motor neuron production are intact.

Ablation of GDE2 after neurogenesis does not impair motor pool formation

At hindlimb levels, GDE2 is first localized to motor neuron cell body areas at the time of motor neuron generation but is subsequently enriched in motor axons from E12.5 (Figure 6B; Figure S5). To define when GDE2 functions in hindlimb motor pool formation, we generated $Gde2^{lox/-}$; $Rosa26:CreER^+$ animals, which enable the timed ablation of GDE2 through Cre-dependent recombination via the administration of 4-hydroxytamoxifen (4-OHT) (Badea et al., 2003). We injected pregnant dams with 4-OHT at E8.5, to ablate GDE2 expression prior to the initiation of motor neuron progenitor differentiation at lumbar levels, and at E10.5 to eliminate GDE2 by the end of motor neuron generation (Nornes and Carry, 1978).

$Gde2^{lox/-}$;$Rosa26:CreER^+$ embryos from pregnant dams injected with 4-OHT at E8.5 or E10.5 showed an equivalent loss of GDE2 in motor neuron cell bodies and axons at E12.5, demonstrating that Cre-mediated loss of GDE2 in both cases had occurred prior to detectable LS2 motor pool formation (Figure 6B, F, D, H; Figure S5). Analysis of the Va, Al, Am and Gp motor pools in $Gde2^{lox/-}$;$Rosa26:CreER^+$ embryos after 4-OHT injection at E8.5 showed a loss of Isl1/2$^+$ motor neurons and a dramatic reduction of ER81$^+$ Va motor neurons at E12.5 and E14.5 compared with $Gde2^{lox/-}$ and $Gde2^{+/-}$; $Rosa26:CreER^+$ controls (Figure 6I–Q; data not shown). Consistent with the phenotype of $Gde2$ null animals, Al, Am and Gp pool formation was delayed such that a decrease in Er81/Isl1$^+$ motor neuron numbers at E12.5 was mitigated by E14.5 (Figure 6I–Q). Thus, elimination of GDE2 prior to the initiation of motor neuron generation mimics the phenotype observed in $Gde2$ null animals. In contrast, administration of 4-OHT at E10.5 did not alter the number of Va, Al, Am or Gp motor neurons in $Gde2^{lox/-}$;$Rosa26:CreER^+$ embryos compared with $Gde2^{lox/-}$ and $Gde2^{+/-}$;$Rosa26:CreER^+$ controls, although the level of GDE2 ablation was equivalent in both cases (Figure 6F, H, K, L, O, P, R; Figure S5).

These results suggest that GDE2 removal at the onset of neurogenesis disrupts the formation of specific motor pools, whereas GDE2 ablation after motor neuron generation is complete does not. Thus, the ability of GDE2 to regulate the formation of specific LMC motor pools coincides precisely with the temporal profile of motor neuron neurogenesis and the localization of GDE2 within motor neuron cell bodies and dendrites.

GDE2 is necessary and sufficient to inhibit Notch signaling

To determine how GDE2 regulates motor neuron differentiation, we considered the possibility that GDE2 might downregulate Notch signaling, a pathway known to be required for the maintenance of Olig2$^+$ motor neuron progenitors in an undifferentiated state (Marklund et al., 2010). To test this hypothesis, we compared the expression of two direct downstream targets of activated Notch in $Gde2^{-/-}$ spinal cords in relation to WT littermates. $Gde2^{-/-}$ animals showed a marked expansion of $Hes5$ and $Blbp$ expression (Figure 7A, B,

D, E); further, GDE2 ablation increased the amount of Notch intracellular domain (NICD) in dissected ventral spinal cords, in accordance with elevated levels of ligand-dependent Notch processing and an increase of activated Notch signaling (Figure 7C; Peng et al., 2007). These data collectively suggest that GDE2 is necessary to downregulate Notch signaling in neighboring motor neuron progenitors. To determine if GDE2 is sufficient to inhibit Notch signaling, we utilized a gain of function approach using in ovo electroporation of embryonic chick spinal cords. Confirming and extending previous studies, overexpression of GDE2 caused Olig2$^+$ progenitors in the VZ to precociously differentiate into Isl2$^+$ motor neurons, while versions of GDE2 mutated within the GDE2 GDPD domain (GDE2.APML) failed to do so (Figure 7F; Rao and Sockanathan, 2005). Embryos electroporated with GDE2 showed a concomitant reduction of *Hes5* and *Blbp* expression, whereas GDE2.APML electroporation did not (Figure 7J–O). These observations suggest that GDE2 is sufficient to inhibit Notch activity and induce motor neuron differentiation, and that this function is dependent on its extracellular GDPD activity. Consistent with this observation, electroporation of a dominant negative (dn) version of the NICD transcriptional coactivator MAML, effectively induced Isl2$^+$ motor neuron differentiation in the VZ synonymous with GDE2 overexpression (Figure 7F–G′; Peng et al., 2007); and coexpression of NICD and GDE2 was sufficient to inhibit GDE2-dependent induction of motor neuron differentiation in VZ progenitors (Figure 7H, I).

GDE2 is expressed in newly differentiating motor neurons in the IZ, predicting that GDE2 functions non cell-autonomously to inhibit Notch signaling in neighboring Olig2$^+$ progenitors. Previous studies have attributed cell- and non cell-autonomous functions for GDE2 in motor neuron differentiation but definitive assessment of GDE2 function is lacking due to insufficient cellular resolution of GDE2-dependent motor neuron differentiation (Rao and Sockanathan, 2005; Yan et al., 2009). To better define the autonomy of GDE2 function at single-cell resolution, we utilized established Cre-lox approaches to drive high levels of GDE2 and LacZ expression in a sparse number of VZ progenitors in the chick spinal cord from bicistronic constructs (Zhuang et al., 2009). We observed a 1:1 correlation with LacZ and GDE2 expression indicating that LacZ is an accurate readout of cells expressing exogenous GDE2 (data not shown). Under these conditions, over 80% of induced Isl2$^+$ neurons in the VZ did not express LacZ but instead were located directly adjacent to LacZ$^+$ cells, suggesting that cell-cell contact is necessary for non cell-autonomous induction of motor neuron differentiation by GDE2 (Figure 7P–R). Further, Isl2$^+$ cells that coexpressed LacZ were only detected when in contact with LacZ$^+$ cells and never in isolation (Figure 7Q, R). Taken together, these observations are consistent with a non cell-autonomous function for GDE2 in triggering motor neuron differentiation.

Discussion

Current models suggest that newly born motor neurons are initially a blank slate in terms of subtype identity, and that motor columnar and pool fates are instructed in these generic new-born motor neurons by Hox transcriptional programs and extrinsically-derived signals (Dasen and Jessell, 2009). Our analyses of GDE2 function prompt these concepts to be reexamined. We show here that GDE2 does not regulate the production of all motor neurons but that GDE2 is required for the timing and formation of motor neurons of defined columnar and pool-specific identities. Strikingly, postmitotic Hox protein expression and activities are not directly affected by GDE2. Instead, GDE2 downregulates Notch signaling pathways in neighboring progenitor cells through a non cell-autonomous mechanism that depends on extracellular GDE2 GDPD activity. This mechanism of GDE2 function is consistent with our observations that ablation of GDE2 decreases progenitor cell-cycle exit, prolongs the mitotic cell-cycle, delays the birth of prospective medially located LMC motor pools, and results in the failure of lateral motor pool formation. Thus, GDE2 regulates the

generation of specific motor neuron subtypes through its role in triggering the differentiation of motor neuron progenitors into postmitotic motor neurons (Figure S6).

These findings have several implications. First, they suggest that signals from postmitotic motor neurons are required for the formation of specific motor neuron subtypes at the level of motor neuron progenitor differentiation, a previously unrecognized concept in existing models of motor neuron diversification. In our model, MMC motor neurons, which are born prior to LMC neurons and do not require GDE2 for their formation, serve as an initial source of GDE2 that regulates the progressive generation of prospective LMC motor neurons from adjacent motor neuron progenitors. This function also applies to forelimb regions, as GDE2 is differentially required for the formation of C7–8 Pea3$^-$ Scip1$^+$ and Pea3$^+$ motor pools (P.S and S.S., unpublished observations). This strategy for building complexity within motor neuron populations is particularly compelling since the MMC is thought to be the ancestral motor column while the LMC is a more recent structure that evolved in accordance with limb development (Fetcho, 1992; Dasen et al., 2008). Feedback signaling mechanisms from postmitotic neurons to progenitor cells have been reported to control differentiation in other structures such as the cortex, where signals from cortical neurons can influence astrocyte generation during the neuronal to glial switch (Namahira et al, 2009; Seuntjens et al., 2009). Our finding that feedback signals also control subtype identity within a single class of neurons suggests that this strategy may form a general mechanism to control cell diversity in the developing nervous system.

A second implication from this study is that newly-born motor neurons are unlikely to be generic as previously believed given their differential requirements for GDE2 for their generation, but are inherently biased towards distinct postmitotic fates. The ability of Hox proteins to alter motor neuron identities in postmitotic motor neurons implies that such fates are not hardwired but are plastic to some degree. We suggest that hierarchical Hox transcriptional programs and additional signals act to consolidate and refine critical columnar and motor pool properties in newly born motor neurons, thus ensuring appropriate connectivity and function of motor circuits over time (Dasen et al., 2003; Dasen et al., 2005; Jung et al., 2010). Conceptually, this model invokes that elements of postmitotic motor neuron identity are encoded in progenitor cells prior to their differentiation into postmitotic motor neurons, and implies that motor neuron progenitors are not uniform but are specified towards distinct postmitotic fates. While our data indicate that such specification includes columnar and pool identities, they also raise the possibility that alpha and gamma motor neuron identities might be encoded within motor neuron progenitors. This hypothesis stems from two observations: first, that the specific loss of LMC alpha motor neurons in postnatal *Gde2*$^{-/-}$ animals correlates with the embryonic phenotype, where the formation of specific LMC motor pools is compromised while MMC motor neurons are unchanged; and second, that the reduction of LMC alpha motor neurons is highly unlikely to be a consequence of altered sensory neuron and interneuron formation in the absence of GDE2, as previous studies show that these neuronal subtypes are dispensable for alpha motor neuron formation and function (reviewed by Grillner and Jessell, 2009). However, further study is required to test this hypothesis as our studies do not exclude alternative interpretations that are independent of progenitor specification, for instance that alpha motor neuron differentiation is predicated on the total number of motor neurons within a motor pool but that gamma motor neuron differentiation is not. Nevertheless, our data collectively suggest that similar to mechanisms that direct the diversification of different neuronal classes within the spinal cord, the acquisition of motor neuron subtype identity is a dynamic and progressive process that is initiated in motor neuron progenitors and continues in postmitotic motor neurons in accordance with their axial position relative to their final targets.

Our analysis of GDE2 function indicates that GDE2 triggers neighboring motor neuron progenitors to undergo differentiation by GDPD inhibition of Notch signaling. Notch signaling maintains the proliferative state of progenitor cells in part by inhibiting the expression of proneural genes such as Mash1 and Ngn2 (reviewed by Corbin et al., 2008). Ngn2 in particular plays pivotal roles in synchronizing neurogenesis and motor neuron specification by decreasing Olig2:Ngn2 ratios to promote neuronal differentiation, and by directly interacting with Lhx3 and Isl1 to regulate the transcription of motor neuron-specific genes (Lee and Pfaff, 2003). Overexpression of GDE2 in the chick spinal cord is sufficient to induce ectopic Ngn2 expression, supporting the model that GDE2 promotes motor neuron differentiation via the derepression of Notch-dependent Ngn2 inhibition (M.R and S.S, unpublished observations). It is widely accepted that Notch signaling plays important roles in generating diversity in neural progenitors. For example, differential Notch activity plays central roles in the sequential specification and binary fate choices of progenitors in the Drosophila peripheral nervous system, as well as in maintaining the heterogeneity of mammalian cortical progenitors (reviewed in Corbin et al., 2008). Accordingly, it is possible that differential Notch signaling could similarly encode aspects of postmitotic motor neuron subtype identity in motor neuron progenitors, and that GDE2-dependent downregulation of Notch signaling could control the differentiation of pool-specific motor neurons. How GDE2 controls the temporal formation of medial LMC neurons via inhibition of Notch signals is less clear. The difference in GDE2 function in terms of regulating the timing of medially located LMC pool formation versus its requirement for the generation of laterally located motor neuron pools correlates with their birthdates, as medial motor pools are born earlier than lateral pools (Nornes and Carry, 1978; Whitelaw and Hollyday, 1983). We speculate that the levels of GDE2 targets might vary over time such that the precise modulation of Notch signaling could directly influence both motor neuron fates and birthdates.

Two major questions that emerge from this work are what are the direct targets of GDE2 GDPD activity, and how do they affect Notch signaling? Definitive identification of GDE2 GDPD substrates is currently underway; however, potential candidates are known from studies in non-neural cells, where GDE2 metabolizes glycerophosphocholine into glycerol-3-phosphate and choline (Gallazzani et al., 2008). However, it is still unclear if glycerophosphocholine is indeed the physiological substrate for GDE2, and if so, how its metabolism could specifically inhibit Notch signaling. Further elucidation of the molecular mechanisms involved will provide key insight into how motor neuron diversity is generated, and may define general principles that underlie the regulation of neuronal differentiation in the developing nervous system.

Experimental Procedures

Generation of Gde2 mutant mice

Linearized targeting constructs were electroporated into 129/Sv ES cells to generate neomycin-resistant clones (Ingenious Targeting Laboratories, Inc.), which were screened for potential recombinants by PCR and then confirmed by Southern blot analysis. A 750bp EcoRI fragment upstream of the targeted region was used as a probe to detect a 4kb WT band and a 2kb band for the correctly targeted allele upon BamH1 digestion. Recombinant clones were injected into C57BL/6J blastocysts to produce chimeric founders, and crossed with C57BL/6J animals to obtain germline transmission. Details of primers used for genotyping are described in supplemental experimental procedures. *Gde2^{lox/+}* mice were bred to lines that express Cre recombinase in germline cells to generate *Gde2^{+/−}* mice. *Gde2^{+/−}* animals were intercrossed to generate *Gde2^{−/−}* null mutants, which were born at the expected Mendelian frequency, and are viable and fertile. Analyses were carried out on

embryos derived from *Gde2*^{+/−} heterozygous intercrosses (mixed 129Sv × C57BL/6J background).

Motor neuron counts

In ovo electroporation of chick embryos was carried out as described in Yan et al., 2009. Cell counts were performed on 10–20 sections from three to five embryos in each instance using Image J software. Details are provided in supplemental experimental procedures.

In situ hybridization and immunofluorescence

In situ hybridization and immunostaining experiments were carried out as described (Rao and Sockanathan, 2005). Confocal images were acquired with a Zeiss LSM 5 PASCAL microscope. The m*Gde2* (680bp) and m*Err3* (776bp) in situ probes were generated from the 3′ UTR region of each gene. Brightfield images were captured on a Zeiss Axioskop2 microscope. Details of antibodies are provided in the supplemental experimental procedures. TUNEL analysis was carried out using the ApopTag fluorescein in situ apoptosis detection kit (Chemicon S7110). Whole-mount GFP staining was performed as described (Huber et. al, 2005) and eGFP-labeled motor axons were visualized in projections of confocal Z-stacks (500–700 μm).

Cell-Cycle Analyses

Cell cycle analyses were performed as described (Yan *et. al*, 2009). Briefly, BrdU (100 mg/kg body weight) was injected intraperitoneally (i.p.) into pregnant females 30min and 16hr prior to embryo harvest for estimation of S-phase and cell-cycle exit indices respectively. To assess S-phase, proliferation index was calculated as $BrdU^+/Ki67^+$ cells where Ki67 marks all cycling cells; cell-cycle exit index as $BrdU^+Ki67^-/BrdU^+Ki67^+$ and mitotic index as $Mpm2^+/Ki67^+$, where Mpm2 marks cells in mitosis (Chenn and Walsh, 2002).

4-OHT injections

4-OHT injections were performed as described (Badea et. al 2003). Briefly, 4-OHT (Sigma) was dissolved in ethanol at a concentration of 20 mg/ml and stored in aliquots at −80°C. Aliquots were emulsified in 5 volumes of sunflower seed oil, centrifuged under vacuum to remove the ethanol, and delivered as a single i.p. injection.

Cell Soma Analysis

Motor neuron cell size measurements were performed on z-series confocal projection images of the LMC at L1–L4 levels. Area measurements were performed using the LSM5 Image examiner software and distribution histograms constructed for each animal by grouping cell body cross sectional areas into 20 μm bins. Average histograms were fit to dual Gaussian distributions using OriginPro8.5 (Origin Labs, USA). From the fitted distributions, average cross-sectional area and standard deviation (SD) of the small and large size MN populations were estimated. The threshold cutoff size for the small population was estimated as the average (μ) + 2 SD (σ) of the fitted small population distribution in control animals of similar age.

Supplementary Material

Refer to Web version on PubMed Central for supplementary material.

Acknowledgments

References

Agalliu D, Takada S, Agalliu I, McMahon AP, Jessell TM. Motor neurons with axial muscle projections specified by Wnt4/5 signaling. Neuron. 2009; 61:708–720. [PubMed: 19285468]

Arber S, Han B, Mendelsohn M, Smith M, Jessell TM, Sockanathan S. Requirement for the homeobox gene Hb9 in the consolidation of motor neuron identity. Neuron. 1999; 23:659–674. [PubMed: 10482234]

Arber S, Ladle DR, Lin JH, Frank E, Jessell TM. ETS gene Er81 controls the formation of functional connections between group Ia sensory afferents and motor neurons. Cell. 2000; 101:485–498. [PubMed: 10850491]

Badea TC, Wang Y, Nathans J. A noninvasive genetic/pharmacologic strategy for visualizing cell morphology and clonal relationships in the mouse. J Neurosci. 2003; 23:2314–2322. [PubMed: 12657690]

Burke RE, Strick PL, Kanda K, Kim CC, Walmsley B. Anatomy of medial gastrocnemius and soleus motor nuclei in cat spinal cord. J Neurophysiol. 1977; 40:667–680. [PubMed: 874534]

Buss RR, Gould TW, Ma J, Vinsant S, Prevette D, Winseck A, Toops KA, Hammarback JA, Smith TL, Oppenheim RW. Neuromuscular development in the absence of programmed cell death: phenotypic alteration of motoneurons and muscle. J Neurosci. 2006; 26:13413–13427. [PubMed: 17192424]

Chenn A, Walsh CA. Regulation of cerebral cortical size by control of cell cycle exit in neural precursors. Science. 2002; 297:365–369. [PubMed: 12130776]

Corbin JG, Gaiano N, Juliano SL, Poluch S, Stancik E, Haydar TF. Regulation of neural progenitor cell development in the nervous system. J Neurochem. 2008; 106:2272–2287. [PubMed: 18819190]

Dasen JS, Liu JP, Jessell TM. MN columnar fate imposed by sequential phases of Hox-c activity. Nature. 2003; 425:926–933. [PubMed: 14586461]

Dasen JS, De Camilli A, Wang B, Tucker PW, Jessell TM. Hox repertoires for motor neuron diversity and connectivity gated by a single accessory factor, FoxP1. Cell. 2008; 134:304–316. [PubMed: 18662545]

Dasen JS, Tice BC, Brenner-Morton S, Jessell TM. A Hox regulatory network establishes motor neuron pool identity and target-muscle connectivity. Cell. 2005; 123:477–491. [PubMed: 16269338]

Dasen JS, Jessell TM. Hox networks and the origins of motor neuron diversity. Curr Top Dev Biol. 2009; 88:169–200. [PubMed: 19651305]

De Marco Garcia NV, Jessell TM. Early motor neuron pool identity and muscle nerve trajectory defined by postmitotic restrictions in Nkx6.1 activity. Neuron. 2008; 57:217–231. [PubMed: 18215620]

Dehay C, Kennedy H. Cell-cycle control and cortical development. Nat Rev Neurosci. 2007; 8:438–450. [PubMed: 17514197]

Diez del Corral R, Olivera-Martinez I, Goriely A, Gale E, Maden M, Storey K. Opposing FGF and retinoid pathways control ventral neural pattern, neuronal differentiation, and segmentation during body axis extension. Neuron. 2003; 40:65–79. [PubMed: 14527434]

Fetcho JR. The spinal motor system in early vertebrates and some of its evolutionary changes. Brain Behav Evol. 1992; 40:82–97. [PubMed: 1422809]

Friese A, Kaltschmidt JA, Ladle DR, Sigrist M, Jessell TM, Arber S. Gamma and alpha motor neurons distinguished by expression of transcription factor Err3. Proc Natl Acad Sci USA. 2009; 106:13588–13593. [PubMed: 19651609]

Gallazzini M, Ferraris JD, Burg MB. GDPD5 is a glycerophosphocholine phosphodiesterase that osmotically regulates the osmoprotective organic osmolyte GPC. Proc Natl Acad Sci USA. 2008; 105:11026–11031. [PubMed: 18667693]

Gutman CR, Ajmera MK, Hollyday M. Organization of motor pools supplying axial muscles in the chicken. Brain Res. 1993; 609:129–136. [PubMed: 8508296]

Grillner S, Jessell TM. Measured motion: searching for simplicity in spinal locomotor networks. Curr Opin Neurobiol. 2009; 19:572–586. [PubMed: 19896834]

Haase G, Dessaud E, Garcès A, de Bovis B, Birling M, Filippi P, Schmalbruch H, Arber S, deLapeyrière O. GDNF acts through PEA3 to regulate cell body positioning and muscle innervation of specific motor neuron pools. Neuron. 2002; 35:893–905. [PubMed: 12372284]

Hollyday M. Organization of motor pools in the chick lumbar lateral motor column. J Comp Neurol. 1980; 194:143–170. [PubMed: 7192292]

Hollyday M, Jacobson RD. Location of motor pools innervating chick wing. J Comp Neurol. 1990; 302:575–588. [PubMed: 1702118]

Huber AB, Kania A, Tran TS, Gu C, De Marco Garcia N, Lieberam I, Johnson D, Jessell TM, Ginty DD, Kolodkin AL. Distinct roles for secreted semaphorin signaling in spinal motor axon guidance. Neuron. 2005; 48:949–964. [PubMed: 16364899]

Hui K, Kucera J, Henderson JT. Differential sensitivity of skeletal and fusimotor neurons to Bcl-2-mediated apoptosis during neuromuscular development. Cell Death Differ. 2008; 15:691–699. [PubMed: 18097449]

Ji SJ, Periz G, Sockanathan S. Nolz1 is induced by retinoid signals and controls motor neuron subtype identity through distinct repressor activities. Development. 2009; 136:231–240. [PubMed: 19056829]

Jung H, Lacombe J, Mazzoni EO, Liem KF Jr, Grinstein J, Mahony S, Mukhopadhyay D, Gifford DK, Young RA, Anderson KV, Wichterle H, Dasen JS. Global control of motor neuron topography mediated by the repressive actions of a single hox gene. Neuron. 2010; 67:781–796. [PubMed: 20826310]

Kanning KC, Kaplan A, Henderson CE. Motor neuron diversity in development and disease. Annu Rev Neurosci. 2010; 33:409–440. [PubMed: 20367447]

Landmesser L. The distribution of motoneurones supplying chick hindlimb muscles. J Physiol. 1978; 284:371–389. [PubMed: 731549]

Landmesser LT. The acquisition of motoneuron subtype identity and motor circuit formation. Int J Dev Neurosci. 2001; 19:175–182. [PubMed: 11255031]

Lee SK, Pfaff SL. Synchronization of neurogenesis and motor neuron specification by direct coupling of bHLH and Homeodomain transcription factors. Neuron. 2003; 38:731–745. [PubMed: 12797958]

Lin JH, Saito T, Anderson DJ, Lance-Jones C, Jessell TM, Arber S. Functionally related motor neuron pool and muscle sensory afferent subtypes defined by coordinate ETS gene expression. Cell. 1998; 95:393–407. [PubMed: 9814709]

Marklund U, Hansson EM, Sundström E, de Angelis MH, Przemeck GK, Lendahl U, Muhr J, Ericson J. Domain-specific control of neurogenesis achieved through patterned regulation of Notch ligand expression. Development. 2010; 137:437–445. [PubMed: 20081190]

Matise MP, Lance-Jones C. A critical period for the specification of motor pools in the chick lumbosacral spinal cord. Development. 1996; 122:659–669. [PubMed: 8625817]

Namahira M, Kohyama J, Semi K, Sanosaka T, Deneen B, Taga T, Nakashima K. Committed neuronal precursors confer astrocytic potential on residual neural precursor cells. Dev Cell. 2009; 16:245–255. [PubMed: 19217426]

Nogusa Y, Fujioka Y, Komatsu R, Kato N, Yanaka N. Isolation and characterization of two serpentine membrane proteins containing glycerophosphodiester phosphodiesterase, GDE2 and GDE6. Gene. 2004; 337:173–179. [PubMed: 15276213]

Nornes HO, Carry M. Neurogenesis in spinal cord of mouse: an autoradiographic analysis. Brain Res. 1978; 159:1–6. [PubMed: 728790]

Novitch BG, Wichterle H, Jessell TM, Sockanathan S. A requirement for retinoic acid-mediated transcriptional activation in ventral neural patterning and motor neuron specification. Neuron. 2003; 40:81–95. [PubMed: 14527435]

Peng CY, Yajima H, Burns CE, Zon LI, Sisodia SS, Pfaff SL, Sharma K. Notch and MAML signaling drives Scl-dependent interneuron diversity in the spinal cord. Neuron. 2007; 53:813–827. [PubMed: 17359917]

Prasad A, Hollyday M. Development and migration of avian sympathetic preganglionic neurons. J Comp Neurol. 1991; 307:237–258. [PubMed: 1713232]

Rao M, Sockanathan S. Transmembrane protein GDE2 induces motor neuron differentiation in vivo. Science. 2005; 309:2212–2215. [PubMed: 16195461]

Rousso DL, Gaber ZB, Wellik D, Morrisey EE, Novitch BG. Coordinated actions of the forkhead protein Foxp1 and Hox proteins in the columnar organization of spinal motor neurons. Neuron. 2008; 59:226–240. [PubMed: 18667151]

Seuntjens E, Nityanandam A, Miquelajauregui A, Debruyn J, Stryjewska A, Goebbels S, Nave KA, Huylebroeck D, Tarabykin V. Sip1 regulates sequential fate decisions by feedback signaling from postmitotic neurons to progenitors. Nat Neurosci. 2009; 12:1373–80. [PubMed: 19838179]

Shah V, Drill E, Lance-Jones C. Ectopic expression of Hoxd10 in thoracic spinal segments induces motoneurons with a lumbosacral molecular profile and axon projections to the limb. Dev Dyn. 2004; 231:43–56. [PubMed: 15305286]

Shneider NA, Brown MN, Smith CA, Pickel J, Alvarez FJ. Gamma motor neurons express distinct genetic markers at birth and require muscle spindle-derived GDNF for postnatal survival. Neural Dev. 2009; 4:42. [PubMed: 19954518]

Thaler JP, Harrison K, Sharma K, Lettieri K, Kehrl J, Pfaff SL. Active suppression of interneuron programs within developing MNs revealed by analysis of homeodomain factor HB9. Neuron. 1999; 23:675–687. [PubMed: 10482235]

Thaler JP, Lee SK, Jurata LW, Gill GN, Pfaff SL. LIM factor Lhx3 contributes to the specification of MN and interneuron identity through cell-type-specific protein-protein interactions. Cell. 2002; 110:237–249. [PubMed: 12150931]

Tsuchida TN, Ensini M, Morton SB, Baldessare M, Edlund T, Jessell TM, Pfaff SL. Topographic organization of embryonic MNs defined by expression of LIM homeobox genes. Cell. 1994; 79:957–970. [PubMed: 7528105]

Vanderhorst VG, Holstege G. Organization of lumbosacral motoneuronal cell groups innervating hindlimb, pelvic floor, and axial muscles in the cat. J Comp Neurol. 1997; 382:46–76. [PubMed: 9136811]

Vrieseling E, Arber S. Target-induced transcriptional control of dendritic patterning and connectivity in motor neurons by the ETS gene Pea3. Cell. 2006; 127:1439–1452. [PubMed: 17190606]

Whitelaw V, Hollyday M. Thigh and calf discrimination in the motor innervation of the chick hindlimb following deletions of limb segments. J Neurosci. 1983; 3:1199–1215. [PubMed: 6854368]

Wu Y, Wang G, Scott SA, Capecchi MR. Hoxc10 and Hoxd10 regulate mouse columnar, divisional and motor pool identity of lumbar motoneurons. Development. 2008; 135:171–182. [PubMed: 18065432]

Yan Y, Sabharwal P, Rao M, Sockanathan S. The antioxidant Prdx1 controls motor neuron differentiation by thiol-redox dependent activation of GDE2. Cell. 2009; 138:1209–1221. [PubMed: 19766572]

Yanaka N, Imai Y, Kawai E, Akatsuka H, Wakimoto K, Nogusa Y, Kato N, Chiba H, Kotani E, Omori K, et al. Novel membrane protein containing glycerophosphodiester phosphodiesterase motif is transiently expressed during osteoblast differentiation. J Biol Chem. 2003; 44:43595–43602. [PubMed: 12933806]

Zhuang B, Su YS, Sockanathan S. FARP1 promotes the dendritic growth of spinal motor neuron subtypes through transmembrane Semaphorin6A and PlexinA4 signaling. Neuron. 2009; 61:359–372. [PubMed: 19217374]

Highlights

- Loss of GDE2 causes selective reduction of LMC and HMC motor neurons.

- GDE2 regulates the timing and formation of specific LMC motor pools.

- GDE2 is required for the differentiation of alpha but not gamma motor neurons.

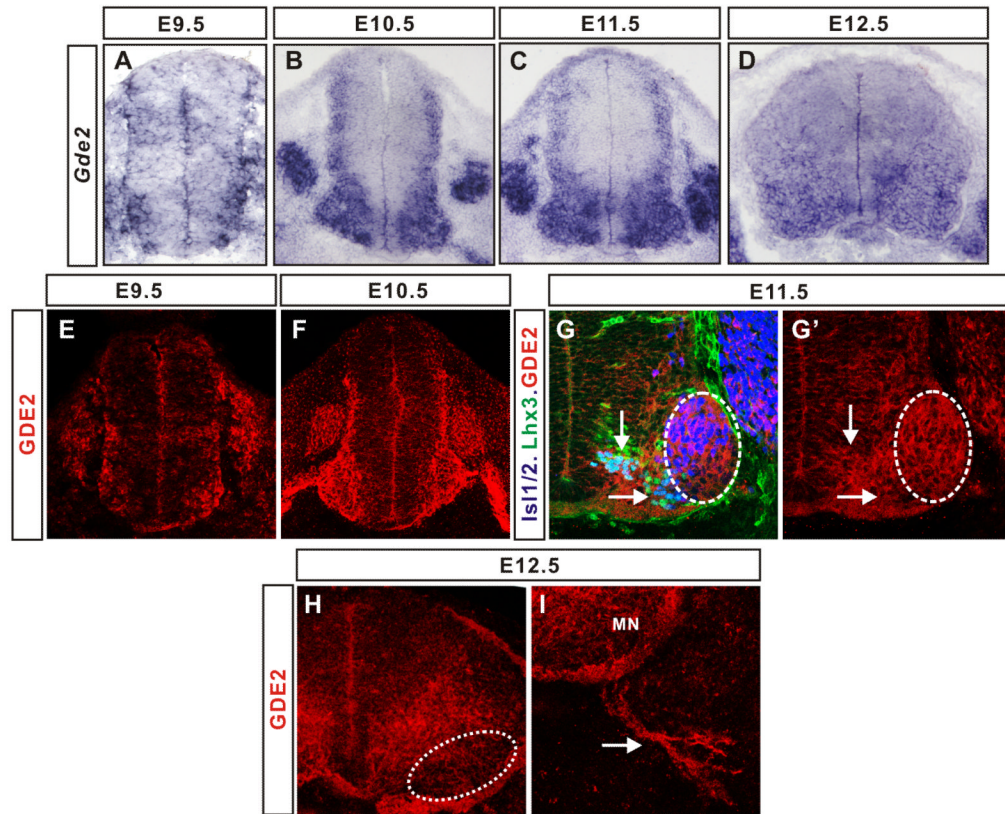- GDE2 inhibits Notch signaling through non cell-autonomous GDPD activity.

Sabharwal et al. Page 15

Figure 1. GDE2 expression in developing motor neurons
(A–D) In situ expression analyses of *Gde2* mRNA on sections of embryonic mouse forelimb spinal cords. *Gde2* transcripts are detected in developing motor neuron cell bodies, dorsal root ganglia and in dorsal-lateral regions of the spinal cord. (E–I) Confocal images of GDE2 protein expression in mouse spinal cord forelimb sections. (G, G′) GDE2 protein expression in relation to motor neuron columnar markers. GDE2 expression alone is shown in G′ for comparison. Vertical arrow=newly differentiating motor neurons; horizontal arrow=MMC, hatched areas=LMC, medially located MMC neurons. (H, I) Hatched circle marks location of motor neurons (MN) in the ventral horn at E12.5, which shows weak GDE2 expression; at this stage, GDE2 is enriched in motor axons (arrow). See also Figure S1.
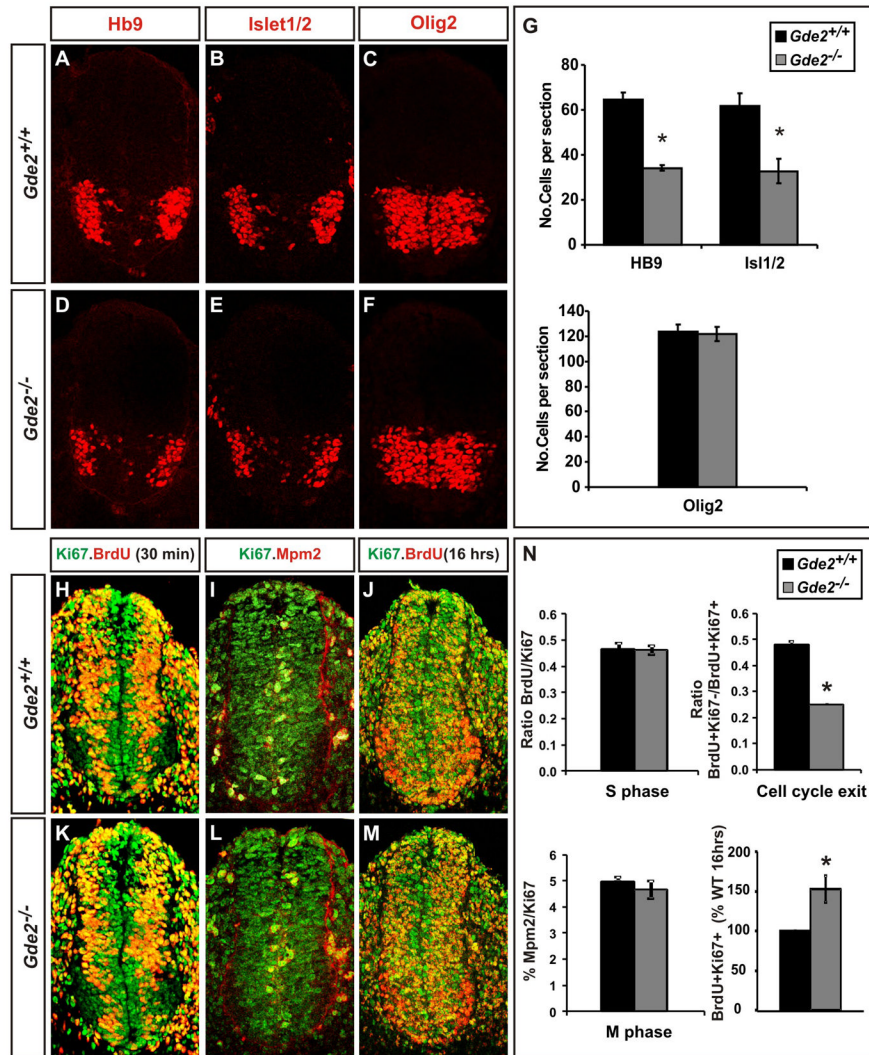
Figure 2. GDE2 is required for motor neuron generation
(A–F; H–M) Confocal images of sections of E9.5 mouse spinal cord. (H, K, J, M) S-phase and cell-cycle exit indices were calculated 30min and 16hrs after BrdU injections respectively. (G) Graphs quantifying HB9$^+$ and Isl1/2$^+$ motor neurons and Olig2$^+$ motor neuron progenitors (HB9 *p= 0.0014; Isl1/2 *p=0.004; Olig2 p= 0.3; n= 5) (N) Graphs of S-phase, M-phase, cell-cycle exit indices and total number of S-phase cells after 16hr BrdU pulse (S-phase p= 0.91; cell-cycle exit *p=0.0005; M-phase p= 0.37; Total S-phase (18hrs) *p= 0.03; n= 4). All graphs: mean ± s.e.m., Student's t-test. See also Figure S2.
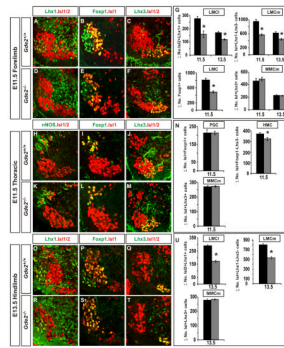
Figure 3. GDE2 function is columnar specific
(A–F; H–M; O–T) Confocal images of ventral left quadrant of sections of E13.5 mouse spinal cords. (G) Graphs quantifying total motor neurons in E11.5 and E13.5 forelimb motor columns (LMCl E11.5 *p= 0.001, E13.5 *p= 0.005; LMCm E11.5 *p=0.002, E13.5 *p= 0.004; LMC E11.5 *p= 0.001; MMC E11.5 p= 0.205, E13.5 p= 0.374). (N) Graphs quantifying total motor neurons in E11.5 thoracic motor columns (PGC p= 0.94; HMC *p= 0.01; MMC p= 0.64) (U) Graphs quantifying total motor neurons in E13.5 hindlimb motor columns (LMCl *p= 0.0004; LMCm *p= 0.0006; MMC p= 0.664). All graphs: mean ± s.e.m., Student's t-test, n= 4. See also Figure S3.
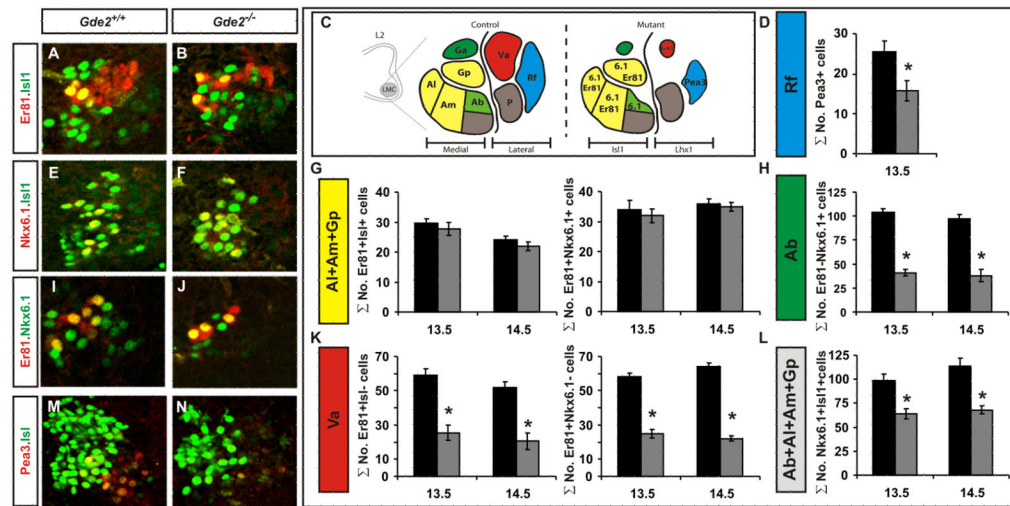
Figure 4. GDE2 function is restricted to specific LMC motor pools
(A, B, E, F, I, J, M, N) Confocal images of ventral left quadrant of E14.5 mouse LS2 spinal cord sections. (C) Schematic of distribution and molecular code of LS2 motor pools. (D, G, H, K, L) Graphs quantifying total motor neurons within E13.5 and E14.5 motor pools (Pea3 *p= 0.0014; Al+Am+Gp [Er81$^+$ Isl1$^+$] E13.5 p= 0.449, E14.5 p= 0.356, [Er81$^+$ Nkx6.1$^+$] E13.5 p= 0.67, E14.5 p= 0.815; Ab [Er81$^-$Nkx6.1$^+$] E13.5 *p= 0.013, E14.5 *p= 0.007; Va [Er81$^+$ Isl1$^-$] E13.5 *p= 0.0001, E14.5 *p= 0.005, [Er81$^+$ Nkx6.1$^-$] E13.5 *p= 0.004, E14.5 *p= 0.002; Ab+Al+Am+Gp E13.5 *p= 0.004, E14.5 *p= 0.006. All graphs: mean ± s.e.m., Student's t-test, E13.5 n= 4, E14.5 n=5. See also Figure S4.
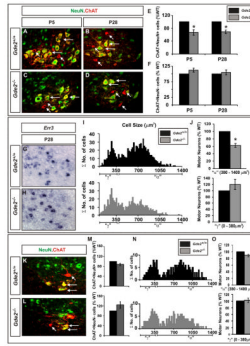
Figure 5. GDE2 is required for LMC alpha motor neuron differentiation
Confocal images of ventral right quadrants of sectioned mouse spinal cords showing lateral (A–D) and medial (K, L) motor neurons. Horizontal arrows: alpha (α) motor neurons. Angled arrows: gamma (γ) motor neurons. (E, F) Graphs quantifying percentage lateral [panel E: P5 *p= 0.009, P28 *p= 0.007; panel F: P5 p= 0.56, P28 p= 0.45] and medial motor neurons [M, Chat$^+$NeuN$^+$ p= 0.09, Chat$^+$NeuN$^-$ p= 0.19]. (G, H) In situ hybridization analyses of sectioned lateral ventral horns of spinal cord. (I) Histograms of somal cell area of ChAT$^+$ lateral motor neurons at P28 (n=845 cells) Average somal areas [mean (μ)]: *Gde2$^{+/+}$*: putative α motor neurons = 703.04μm^2 ± 196.64 [SD (σ)], putative γ motor neurons = 239.47 μm^2 ± 69.7; *Gde2$^{-/-}$*: putative α motor neurons = 609.04μm^2 ± 210.17, putative γ motor neurons = 246.34μm^2 ± 96.4. (J, O) Graphs quantifying percentage putative γ and α motor neurons according to somal area. Threshold cutoff sizes for lateral and medial γ motor neuron populations were estimated as 380μm^2 in cell area (μ + 2σ of the fitted small population distribution in controls); panel J α motor neurons *p= 0.0004; γ motor neurons p= 0.3; panel O α motor neurons p= 0.69; γ motor neurons p= 0.1. (N) Histograms of somal cell area of ChAT$^+$ medial motor neurons at P28 (n= 229 cells) Average somal areas: *Gde2$^{+/+}$*: putative α motor neurons = 818.33μm^2 ± 196, putative γ motor neurons = 268.05 μm^2 ± 84.56; *Gde2$^{-/-}$*: putative α motor neurons = 794.51 μm^2 ± 207.93, putative γ motor neurons = 267.36 μm^2 ± 86.68. All graphs: mean ± s.e.m., One sample t-test, n= 4.
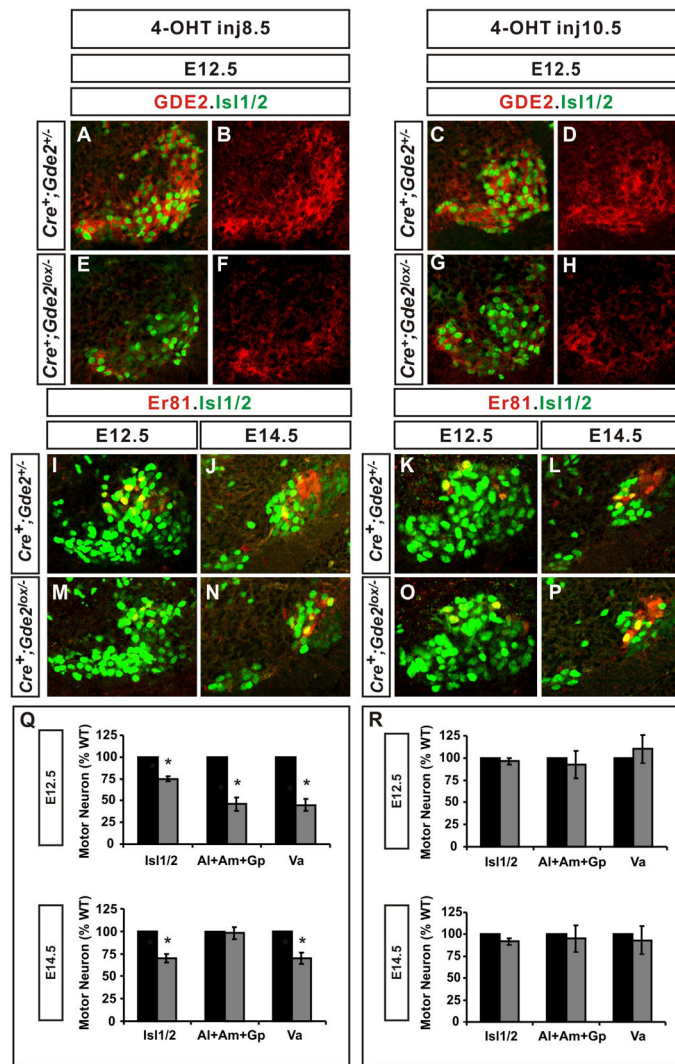
Figure 6. GDE2 functions during the period of motor neuron generation
(A–P) Confocal images of ventral right quadrant of mouse LS2 spinal cord sections at E12.5 except where stated. (Q, R) Graphs quantifying the percentage motor neurons within E12.5 and E14.5 motor pools, black bar: $Cre^+; Gde2^{+/−}$, grey bar: $Cre^+; Gde2^{lox/−}$ [panel Q: E12.5 Isl1/2 *p= 0.0002, Al+Am+Gp *p= 0.007, Va *p= 0.001; E14.5 Isl1/2 *p= 0.0017, Al +Am+Gp p= 0.75, Va *p= 0.02. panel R: E12.5 Isl1/2 p= 0.382, Al+Am+Gp p= 0.509, Va p= 0.761; E14.5 Isl1/2 p= 0.255, Al+Am+Gp p= 0.477, Va p= 0.676]. All graphs: mean ± s.e.m., One sample t-test, n= 3. See also Figure S5.
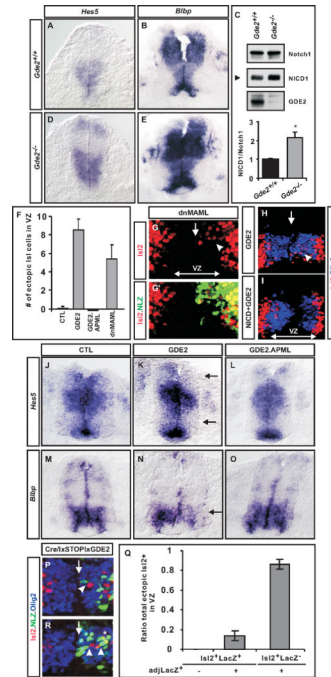
Figure 7. GDE2 inhibits Notch signaling
In situ hybridizations of transverse sections of E9.5 (A, D) and E10.5 (B, E) mouse and electroporated chick spinal cords at HH St 19 (J–O) showing expression of *Hes5* and *Blbp* transcripts. Arrows mark areas of Notch inhibition. (C) Western blot of dissected E10.5 spinal cord extracts from $Gde2^{-/-}$ embryos and WT littermates. Graph shows densitometric quantitation of NICD/full length Notch ratios from Western blots *p= 0.035, n=4. (F) Graph shows average number of ectopic Isl2$^+$ motor neurons/section in VZ of electroporated chick spinal cords, n=8–10. (G, G′, H, I) Confocal images of transverse sections of chick spinal cords electroporated on the right; VZ, ventricular zone; vertical arrow, midline. Arrowheads mark ectopic Isl2$^+$ motor neurons. (P, R) Two examples of chick spinal cords electroporated on the right with Lox-STP-Lox GDE2, and CMV:Cre plasmids. Green cells express GDE2; neighboring red cells are progenitors that have differentiated into Isl2$^+$ motor neurons. * in R marks Isl2$^+$ cells expressing GDE2. (Q) Graph quantifying ectopic Isl2$^+$ motor neurons with respect to LacZ GDE2$^+$ cells n= 161 cells. All graphs: mean ± s.e.m., Student's t-test. Statistical analyses using a simple binomial distribution showed that the results we obtain cannot be explained by chance (see supplemental methods). See also Figure S6.